



# Emergence of coherent oscillations in stochastic models for circadian rhythms

Didier Gonze, José Halloy, Albert Goldbeter\*

*Unité de Chronobiologie Théorique, Faculté des Sciences, Université Libre de Bruxelles, Campus Plaine, C.P. 231, B-1050 Brussels, Belgium*

Received 18 December 2003; received in revised form 19 January 2004

Available online 17 May 2004

---

## Abstract

Most living organisms have developed the capability of generating autonomously sustained oscillations with a period close to 24 h. The mechanism responsible for these circadian rhythms relies on the negative regulation exerted by a protein on the expression of its own gene. Deterministic models for circadian rhythms account for the occurrence of autonomous oscillations of the limit cycle type, for their entrainment by light–dark cycles, and for their phase shifting by light pulses. Such models, however, do not take into consideration the molecular fluctuations which arise when the number of molecules involved in the regulatory mechanism is low. Here we resort to a stochastic description of a core model for circadian rhythms to study the emergence of coherent oscillations in gene expression in the presence of molecular noise. We show that despite the “bar code” pattern of gene activation, robust circadian oscillations can be observed. Simulations of the deterministic, fully developed version of the circadian model indicate, however, that sustained oscillations only emerge above a critical value of the rate constants characterizing the reversible binding of repressor to the gene, while below this value the system evolves towards an excitable steady state. This explains why, depending on whether or not the critical value of these rate constants is exceeded, stochastic simulations of the model produce coherent oscillations or very noisy oscillations with a highly variable period.

© 2004 Elsevier B.V. All rights reserved.

PACS: 80; 87; 87.16.–b; 87.16.yc

Keywords: Circadian rhythms; Stochastic simulations; Molecular noise

---

\* Corresponding author. Tel.: 32-2-650-5772; fax: 32-2-650-5767.  
E-mail address: [agoldbet@ulb.ac.be](mailto:agoldbet@ulb.ac.be) (A. Goldbeter).

## 1. Introduction

To adapt physiological behavior to the natural alternation of day and night, most living organisms have developed the capability of generating autonomously sustained oscillations with a period close to 24 h. These circadian rhythms are endogenous because they can occur in constant environmental conditions (e.g. constant darkness). During the last decade experimental studies have shed much light on the molecular mechanism of circadian rhythms [1–3]. In all eukaryotic organisms, the molecular mechanism of circadian oscillations relies on the negative feedback exerted by a clock protein on the expression of its gene [1–4]. Based on these experimental observations, mathematical models for circadian rhythms have been proposed [5–12]. Taking the form of a system of coupled ordinary differential equations, these deterministic models predict that, in a certain range of parameter values, the genetic regulatory network can produce sustained oscillations of the limit cycle type.

One limitation of deterministic models is that they do not take into consideration the fact that the number of molecules involved in the regulatory mechanism within the rhythm-producing cells may be low. At low concentrations of protein or messenger RNA molecules, molecular fluctuations are likely to have a marked impact on circadian oscillations [13]. To assess the effect of molecular noise, it is necessary to resort to a stochastic approach. In previous work [14–16], we compared the predictions of deterministic and stochastic versions of a core model for circadian rhythms and showed that robust circadian oscillations can be observed already when the maximum number of mRNA and protein molecules is of the order of some tens and hundreds, respectively.

Here we study in more detail the stochastic dynamics of circadian oscillations, focusing on the role of gene expression. After describing the deterministic and stochastic versions of the model, we show how robust circadian oscillations are produced from a “bar-code” pattern of gene expression. We focus on the effect of the association and dissociation rate constants characterizing the binding of the repressor protein to the gene, and show that coherent oscillations only emerge once these parameters exceed a critical value.

## 2. Description of the stochastic model for circadian oscillations

For our analysis, we resort to a five-variable model proposed for circadian oscillations of the PER protein and *per* mRNA in *Drosophila* [5,6,14]. This core model could also apply to the FRQ oscillator in *Neurospora* [8]. Extensions of this one-feedback loop model for *Drosophila* [7–9] and mammals [10] have also been proposed. The model, schematized in Fig. 1, is based on the negative feedback exerted by a protein on the expression of its gene. The gene is first expressed in the nucleus and transcribed into messenger RNA (mRNA). The latter is transported into the cytosol where it is degraded and translated into the protein  $P_0$ . This protein undergoes reversible phosphorylation, from  $P_0$  into  $P_1$  and from  $P_1$  into  $P_2$ . The fully phosphorylated form of the protein is marked up for degradation, and transported into the nucleus in a reversible manner. The nuclear form of the protein ( $P_N$ ) represses the transcription of

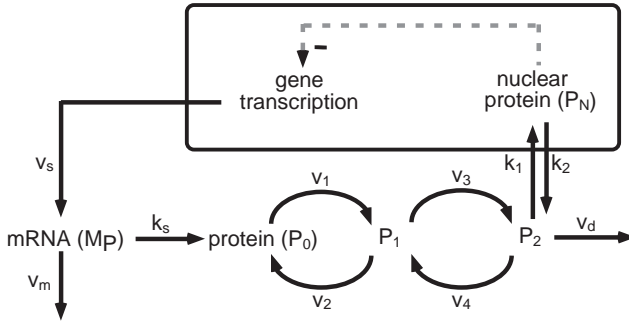


Fig. 1. Scheme of the core molecular model for circadian rhythms [5,6], based on the negative feedback exerted by a protein on the expression of its gene (see text).

the gene. Phosphorylation, dephosphorylation, and degradation steps are assumed to obey Michaelian kinetics, and repression is supposed to be cooperative.

In this core model for circadian rhythms [5,6], the temporal variation of the concentrations of mRNA ( $M_P$ ) and of the various forms of the regulatory protein, cytosolic ( $P_0, P_1, P_2$ ) or nuclear ( $P_N$ ), is governed by the following deterministic system of five kinetic equations (see [5,6] for further details and definition of the parameters):

$$\frac{dM_P}{dt} = v_s \frac{K_I^n}{K_I^n + P_N^n} - v_m \frac{M_P}{K_m + M_P}, \tag{1}$$

$$\frac{dP_0}{dt} = k_s M_P - v_1 \frac{P_0}{K_1 + P_0} + v_2 \frac{P_1}{K_2 + P_1}, \tag{2}$$

$$\frac{dP_1}{dt} = v_1 \frac{P_0}{K_1 + P_0} - v_2 \frac{P_1}{K_2 + P_1} - v_3 \frac{P_1}{K_3 + P_1} + v_4 \frac{P_2}{K_4 + P_2}, \tag{3}$$

$$\frac{dP_2}{dt} = v_3 \frac{P_1}{K_3 + P_1} - v_4 \frac{P_2}{K_4 + P_2} - v_d \frac{P_2}{K_d + P_2} - k_1 P_2 + k_2 P_N, \tag{4}$$

$$\frac{dP_N}{dt} = k_1 P_2 - k_2 P_N. \tag{5}$$

This model accounts for the occurrence of sustained circadian oscillations in continuous darkness [5,6]. Similar results have been obtained in more detailed models incorporating additional clock gene products [7–10]. To assess the effect of molecular noise on the temporal evolution of the genetic control system, we decomposed the latter into “elementary” reaction steps (see Table 1) and performed numerical simulations by means of the Gillespie method [17,18]. In this approach, a parameter denoted  $\Omega$  allows us to control the number of molecules present in the system.

### 3. Deterministic versus stochastic circadian oscillations

Numerical simulations of the deterministic Eqs. (1)–(5) show that in a certain range of parameter values sustained oscillations with a period close to 24 h occur (Fig. 2B).

Table 1  
Description of the stochastic model for circadian rhythms [16,17]

Reaction number	Reaction step	Probability of reaction step
1a	$G + P_N \xrightarrow{a_1} GP_N$	$w_1 = a_1 \times G \times P_N / \Omega$
1b	$GP_N \xrightarrow{d_1} G + P_N$	$w_2 = d_1 \times GP_N$
1c	$GP_N + P_N \xrightarrow{a_2} GP_{N2}$	$w_3 = a_2 \times GP_N \times P_N / \Omega$
1d	$GP_{N2} \xrightarrow{d_2} GP_N + P_N$	$w_4 = d_2 \times GP_{N2}$
1e	$GP_{N2} + P_N \xrightarrow{a_3} GP_{N3}$	$w_5 = a_3 \times GP_{N2} \times P_N / \Omega$
1f	$GP_{N3} \xrightarrow{d_3} GP_{N2} + P_N$	$w_6 = d_3 \times GP_{N3}$
1g	$GP_{N3} + P_N \xrightarrow{a_4} GP_{N4}$	$w_7 = a_4 \times GP_{N3} \times P_N / \Omega$
1h	$GP_{N4} \xrightarrow{d_4} GP_{N3} + P_N$	$w_8 = d_4 \times GP_{N4}$
1i	$[G, GP_N, GP_{N2}, GP_{N3}] \xrightarrow{v_s} MP$	$w_9 = v_s \times (G + GP_N + GP_{N2} + GP_{N3})$
2a	$MP + E_m \xrightarrow{k_{m1}} C_m$	$w_{10} = k_{m1} \times MP \times E_m / \Omega$
2b	$C_m \xrightarrow{k_{m2}} MP + E_m$	$w_{11} = k_{m2} \times C_m$
2c	$C_m \xrightarrow{k_{m3}} E_m$	$w_{12} = k_{m3} \times C_m$
3	$MP \xrightarrow{k_s} MP + P_0$	$w_{13} = k_s \times MP$
4a	$P_0 + E_1 \xrightarrow{k_{11}} C_1$	$w_{14} = k_{11} \times P_0 \times E_1 / \Omega$
4b	$C_1 \xrightarrow{k_{12}} P_0 + E_1$	$w_{15} = k_{12} \times C_1$
4c	$C_1 \xrightarrow{k_{13}} P_1 + E_1$	$w_{16} = k_{13} \times C_1$
5a	$P_1 + E_2 \xrightarrow{k_{21}} C_2$	$w_{17} = k_{21} \times P_1 \times E_2 / \Omega$
5b	$C_2 \xrightarrow{k_{22}} P_1 + E_2$	$w_{18} = k_{22} \times C_2$
5c	$C_2 \xrightarrow{k_{23}} P_0 + E_2$	$w_{19} = k_{23} \times C_2$
6a	$P_1 + E_3 \xrightarrow{k_{31}} C_3$	$w_{20} = k_{31} \times P_1 \times E_3 / \Omega$
6b	$C_3 \xrightarrow{k_{32}} P_1 + E_3$	$w_{21} = k_{32} \times C_3$
6c	$C_3 \xrightarrow{k_{33}} P_2 + E_3$	$w_{22} = k_{33} \times C_3$
7a	$P_2 + E_4 \xrightarrow{k_{41}} C_4$	$w_{23} = k_{41} \times P_2 \times E_4 / \Omega$
7b	$C_4 \xrightarrow{k_{42}} P_2 + E_4$	$w_{24} = k_{42} \times C_4$
7c	$C_4 \xrightarrow{k_{43}} P_1 + E_4$	$w_{25} = k_{43} \times C_4$
8a	$P_2 + E_d \xrightarrow{k_{d1}} C_d$	$w_{26} = k_{d1} \times P_2 \times E_d / \Omega$
8b	$C_d \xrightarrow{k_{d2}} P_2 + E_d$	$w_{27} = k_{d2} \times C_d$
8c	$C_d \xrightarrow{k_{d3}} E_d$	$w_{28} = k_{d3} \times C_d$
9	$P_2 \xrightarrow{k_1} P_N$	$w_{29} = k_1 \times P_2$
10	$P_N \xrightarrow{k_2} P_2$	$w_{30} = k_2 \times P_N$

The five-variable model described by Eqs. (1)–(5) has been decomposed into 30 “elementary” steps. The probability  $w_i$  of each reaction is directly related to the kinetic parameters defined in the deterministic version. Steps (1a–h) pertain to the formation and dissociation of the various complexes between the gene promoter and nuclear protein ( $P_N$ ).  $G$  denotes the unliganded promoter of the gene, while  $GP_N, GP_{N2}, GP_{N3}$  and  $GP_{N4}$  denote the complexes formed by the gene promoter with 1, 2, 3 or 4  $P_N$  molecules. Step (1i) relates to the active state of the promoter leading to expression of the gene and synthesis of mRNA ( $MP$ ). In the case considered we assume that only the complex between the promoter and four molecules of  $P_N$  is inactive. Steps (2) pertain to the degradation of  $MP$  by enzyme  $E_m$ , through formation of the complex  $C_m$ . Step (3) relates to synthesis of unphosphorylated clock protein ( $P_0$ ) at a rate proportional to the number of mRNA molecules. Steps (4) refer to the phosphorylation of  $P_0$  into  $P_1$  by kinase  $E_1$ , through formation of complex  $C_1$ . Steps (5) refer to the dephosphorylation of  $P_1$  into  $P_0$  by phosphatase  $E_2$ , through formation of complex  $C_2$ . Steps (6) and (7) pertain to the corresponding phosphorylation of  $P_1$  into  $P_2$  and dephosphorylation of  $P_2$  into  $P_1$ . Steps (8) relate to the degradation of the phosphorylated form  $P_2$  by enzyme  $E_d$ , through formation of complex  $C_d$ . Steps (9) and (10) refer, respectively, to entry of  $P_2$  into and exit of  $P_N$  from the nucleus.

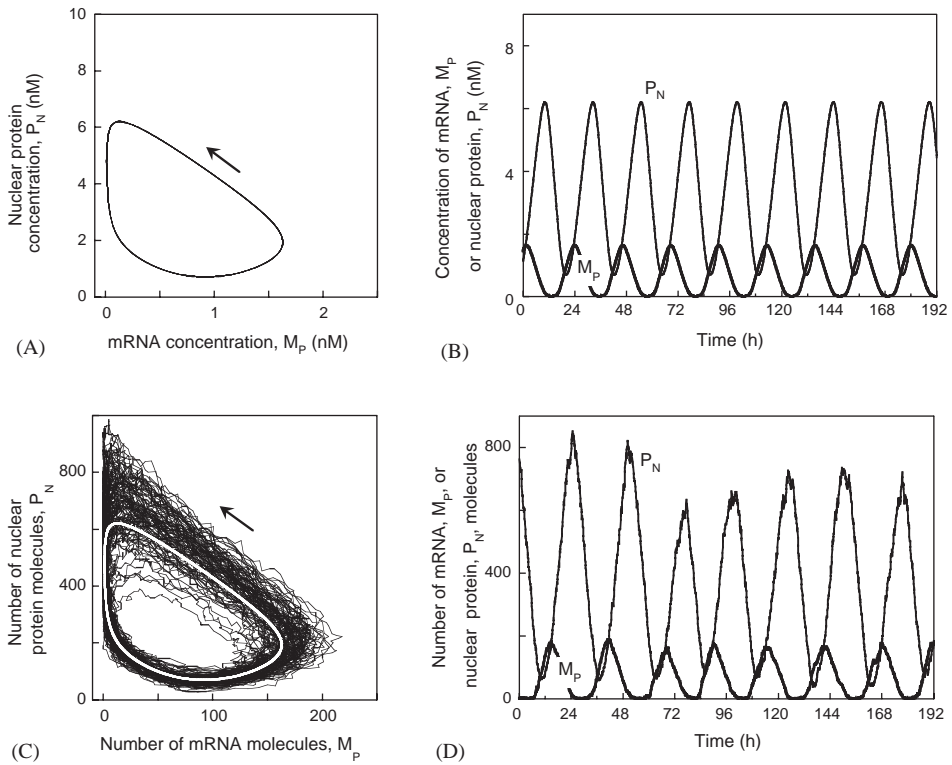


Fig. 2. Sustained circadian oscillations and limit cycles predicted by the deterministic and stochastic versions of the core model for circadian rhythms. (A) Limit cycle and (B) oscillations obtained in the 5-variable deterministic model governed by Eqs. (1)–(5), shown as a projection onto the  $P_N - M_P$  phase plane. (C) Limit cycle and (D) oscillations obtained for the stochastic model listed in Table 1 by means of the Gillespie method. In (C), the deterministic limit cycle obtained in (A) in corresponding conditions is shown as a thick white curve. Concentrations are transformed into numbers of molecules through multiplication by parameter  $\Omega$ , which is equal to 100. Other parameter values are listed in Table 2.

These oscillations correspond to the evolution toward a limit cycle shown in Fig. 2A as a projection onto the plane formed by the concentrations of mRNA ( $M_P$ ) and nuclear clock protein ( $P_N$ ). Oscillations obtained by applying the Gillespie algorithm are shown in Fig. 2D, while the corresponding trajectory in the phase plane is represented in Fig. 2C. To highlight the link between the deterministic and stochastic behaviors, we represented in Fig. 2C the deterministic limit cycle as a thick white curve. The effect of molecular noise is merely to spread the limit cycle trajectory [14]. This noise-induced spreading affects both the amplitude and the period of the oscillations. The results further indicate that robust circadian oscillations are still produced by the stochastic model when the maximum numbers of mRNA and protein molecules are in the order of tens and hundreds, respectively. It is only when these numbers decrease down to a few tens that noise begins to overcome rhythmic behavior, even though somewhat regular oscillations still subsist [14–16].

#### 4. Emergence of coherent oscillations from a bar-code pattern of gene expression

Among all the 30 reaction steps taking place in the core model, regulation of gene expression is described by the successive binding of four molecules of nuclear protein  $P_N$  to the single copy of gene  $G$ ; only the gene bound to four  $P_N$  molecules is considered to be inactive. The active form of the gene,  $G^*$ , thus takes into account the forms  $G$ ,  $GP_N$ ,  $GP_{N2}$ , and  $GP_{N3}$ ;  $G^* = 0$  means that the gene is in the inactive form  $GP_{N4}$ , while  $G^* = 1$  means that the gene can be transcribed, with a probability equal to  $v_s$ . When the number of  $P_N$  molecules is low, the gene can stay active during a long time and this gives rise to an increase in mRNA amount. When the number of  $P_N$  molecules is high, the gene undergoes numerous transitions between the active and inactive forms, due to rapid binding and unbinding of the inhibitory protein. In this case, the propensity for the gene to be transcribed is weaker, and mRNA is decreasing.

Gene activity thus takes the form of a “bar-code” pattern, as shown by Fig. 3. In (A) a peak is drawn each time a molecule of mRNA is produced by step (1i)

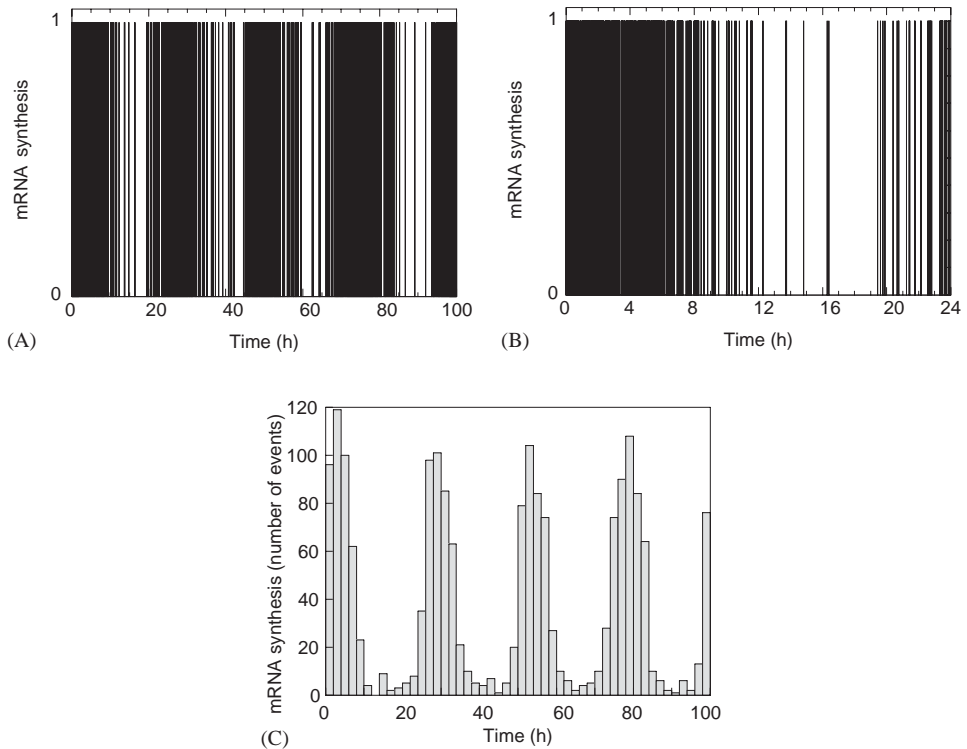


Fig. 3. Stochastic dynamics of gene expression. Each peak in (A) indicates that one transcriptional event leading to mRNA synthesis takes place. In (B) similar results are shown, on an enlarged scale, over one circadian period. Individual events of gene expression are grouped over 2-h intervals in (C), revealing the emergence of circadian oscillations. Parameter values are given in Table 2.

(see Table 1). In (B) the time course of gene expression over one circadian period shows that transcriptional events do not occur in a uniform way during this time interval. The oscillatory pattern appears even more clearly when we group transcription events that occur during intervals of 2 h (C). This representation reveals the emergence of a circadian variation in gene activity.

### 5. Effect of the rate constants characterizing repressor binding to the gene

We previously showed that the proximity of a bifurcation point increases the magnitude of fluctuations around the deterministic limit cycle [15,16]. In these studies, we chose the maximum protein degradation rate,  $v_d$ , as the control parameter because in *Drosophila* light is known to reset the circadian clock through protein degradation [1–3]. Here, we study the effect of varying parameters  $a_i$  and  $d_i$  which represent the rate constants for association and dissociation of nuclear protein molecules ( $P_N$ ) to the gene ( $G$ ). To this end, we divided  $a_i$  and  $d_i$  ( $i = 1-4$ ) by a scaling factor,  $\gamma$ . In Fig. 4 are shown the results of stochastic simulations of the

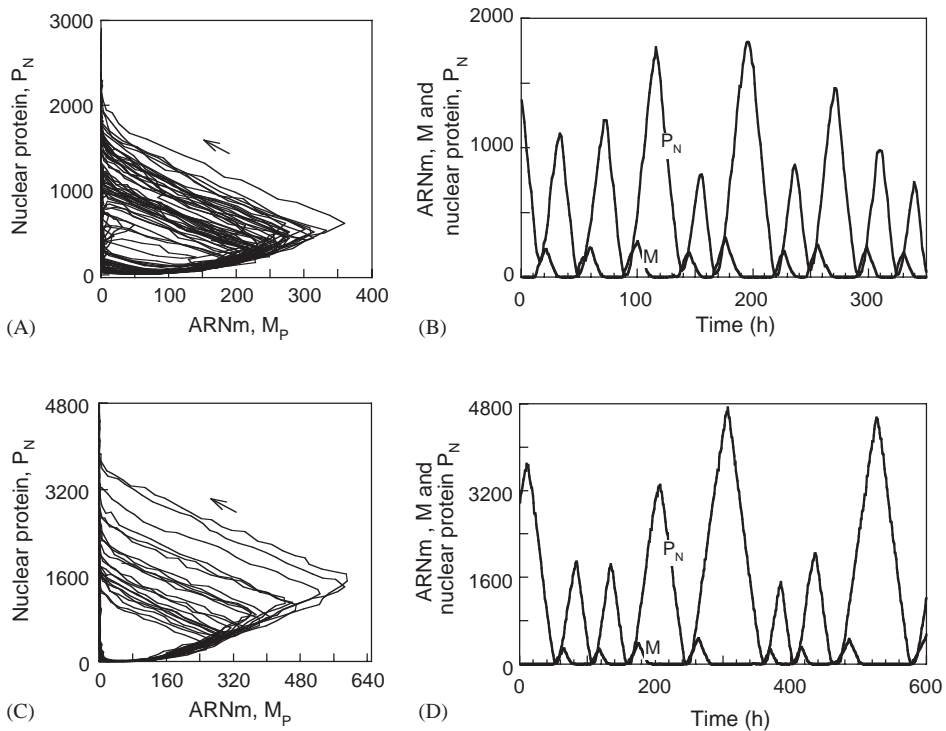


Fig. 4. Trajectory in the phase space and irregular time series obtained by stochastic simulations of the core model for circadian rhythms, for  $\gamma = 100$  (A and B) and  $\gamma = 1000$  (C and D). The curves were obtained for  $\Omega = 100$ ; other parameter values are given in Table 2. The results should be compared with those obtained in Fig. 6 for the corresponding, fully developed version of the deterministic model given in appendix.

model of Table 1 for  $\gamma = 100$  (panels A and B) and  $\gamma = 1000$  (panels C and D). As  $\gamma$  increases up to 100 and 1000, oscillations with larger and larger amplitude and increasing variability of the period are observed. The oscillations obtained for  $\gamma = 1$  are much more regular, as shown in Figs. 2C and D.

To clarify the nature of this phenomenon, it is useful to consider the deterministic version of the detailed stochastic model considered in Table 1. To the 30 reaction steps listed in Table 1 corresponds a deterministic system of 22 ordinary differential equations (see appendix). Because the deterministic model is continuous, variables  $G$ ,  $GP_N$ ,  $GP_{N2}$ ,  $GP_{N3}$  and  $GP_{N4}$  can now take all real intermediate values between 0 and 1. In this fully developed version of the deterministic model, parameters  $a_i$  and  $d_i$  appear explicitly, while they only appear in the form of a single equilibrium inhibition constant,  $K_I$ , in the reduced 5-variable deterministic model governed by Eqs. (1)–(5).

The results obtained with the fully developed deterministic model demonstrate the existence of a bifurcation as a function of the scaling parameter  $\gamma$ , as shown by the bifurcation diagram in Fig. 5. When  $\gamma$  increases above a critical value close to 100, the system ceases to oscillate and evolves toward a stable steady state. In Fig. 6 we compare numerical simulations performed with the 22-variable deterministic model for  $\gamma = 1000$ , 100 and 1. For  $\gamma = 1$  (E and F), large amplitude oscillations are observed. For  $\gamma = 100$  (C and D), the system still undergoes sustained, low-amplitude oscillations. For  $\gamma = 1000$  (A and B), the system evolves towards a stable steady state, but this steady state is excitable: a small perturbation bringing the system slightly away from the steady state triggers a large excursion in the phase space, which corresponds to a burst of transcriptional activity, before the system returns to the stable steady state. This property of excitability also holds for the limit cycle observed for  $\gamma = 100$  (C and D). Thus, it is also possible to trigger large-amplitude peaks in gene transcription starting from such small-amplitude oscillations.

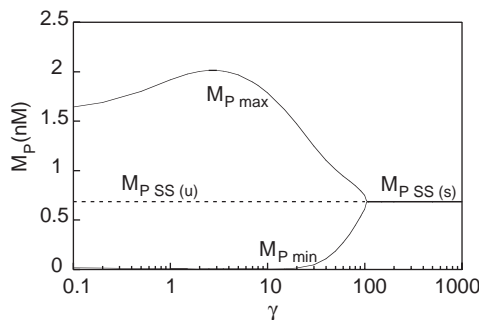


Fig. 5. Bifurcation diagram showing the onset of circadian oscillations in the deterministic model as a function of the scaling parameter  $\gamma$ , which divides the association and dissociation rate constants  $a_i$  and  $d_i$  characterizing the binding of the repressor protein to the gene. The curve shows the steady-state level of mRNA, stable (solid line,  $M_{P,SS(s)}$ ) or unstable (dashed line,  $M_{P,SS(u)}$ ), as well as the maximum ( $M_{P,max}$ ) and minimum ( $M_{P,min}$ ) mRNA concentration in the course of sustained oscillations. The diagram was determined by numerical integration of Eqs. (A.1)–(A.22) for the fully developed deterministic model (see appendix). Parameter values are given in Table 2.

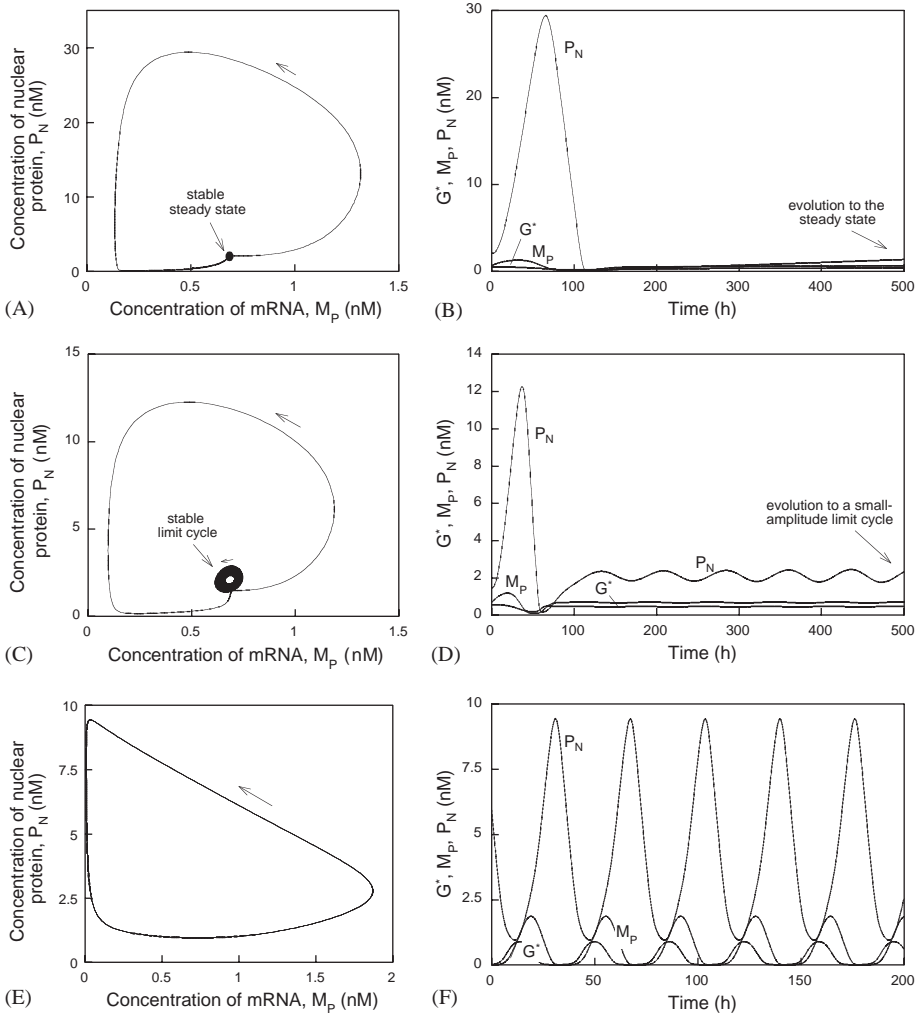


Fig. 6. Emergence of coherent circadian oscillations as a function of scaling parameter  $\gamma$ . The curves were obtained for the fully developed deterministic model, by numerical integration of Eqs. (A.1)–(A.22) listed in appendix. (A) Trajectory in phase space, and (B) time evolution of the system, for  $\gamma = 1000$ , from an initial condition close to the stable steady state. Because the latter is excitable, the trajectory first makes a large excursion in phase space before returning to steady state. (C) Small-amplitude limit cycle and (D) corresponding sustained oscillations for  $\gamma = 100$ . (E) Large-amplitude limit cycle and (F) corresponding sustained oscillations for  $\gamma = 1$ . The latter case pertains to the situation predicted in Fig. 2 for the reduced, 5-variable deterministic model. Parameter values are given in Table 2.

These results explain why oscillations predicted by stochastic simulations become highly irregular when the rate constants  $a_i$  and  $d_i$  decrease below a critical value: as shown by the study of the corresponding detailed deterministic model, such irregular oscillations reflect repetitive, noise-induced large excursions away from a stable,

excitable steady state or from a small-amplitude limit cycle close to the bifurcation point. When  $\gamma$  decreases, i.e., when the values of parameters  $a_i$  and  $d_i$  increase—as in the case considered in Figs. 2C and D, which corresponds to  $\gamma = 1$ —the oscillations become more regular and more robust, because the system operates well into the domain of sustained, large-amplitude oscillations.

## 6. Discussion

Previous comparison of deterministic and stochastic versions of a core model for circadian rhythms based on negative autoregulation of gene expression showed that this regulatory mechanism can produce robust circadian oscillations already when the maximum number of protein and mRNA molecules is of the order of hundreds or tens, respectively [14–16]. It is only at very low numbers of molecules of protein and mRNA that noise begins to obliterate circadian periodicity. Here we focused on the emergence of coherent oscillations in the stochastic dynamics of gene activation and showed that even though gene activation undergoes rapid fluctuations between an active and an inactive state, giving rise to a “bar-code”-like pattern, circadian behavior emerges when grouping transcription events that occur within a finite time interval, e.g. of 2 h. Thus rapid gene activation on a short time scale, of the order of seconds or minutes, leads to robust oscillations with a period of 24 h.

We also analyzed the effect of varying the rate constants characterizing the reversible binding of the repressor protein to the gene. A study of a fully developed version of the deterministic model, in which these parameters appear explicitly, shows that below a certain threshold value of these rate constants the system evolves toward an excitable steady state. In the same conditions the stochastic simulations of the model produce highly noisy oscillations with a great variability of the period. This behavior can be compared to the results obtained by Vilar et al. [19]. Using a two-feedback loop model these authors showed that, for parameter values giving rise to an excitable steady state, highly variable oscillations are produced by the stochastic simulations. The occurrence of such erratic oscillations is mainly due to the absence of a limit cycle attractor. A stable limit cycle stabilizes the oscillations by damping the noise-induced fluctuations [20].

The maximum value of the bimolecular association rate constants  $a_i$  ( $i = 1, \dots, 4$ ) considered in Fig. 2 goes from  $10^3$  to  $5 \times 10^4$  molecule<sup>-1</sup> h<sup>-1</sup> for  $\Omega$  ranging from 10 to 500 (see Table 2). For a nuclear volume of  $10^{-13}$  l, for which a concentration of 1 nM corresponds to 60 molecule per nucleus, these values of  $a_i$  correspond to values of the bimolecular rate constants ranging from  $1.5 \times 10^{10}$  to  $7.5 \times 10^{11}$  M<sup>-1</sup> s<sup>-1</sup>. Such values are larger than the diffusion limit of  $10^8$ – $10^9$  M<sup>-1</sup> s<sup>-1</sup> usually considered for bimolecular rate constants. However, values of up to  $10^{10}$  M<sup>-1</sup> s<sup>-1</sup> [21,22] or even higher values [23] characterize the binding of a repressor to the gene promoter because of a “facilitated diffusion” process mediated by encounter of the protein with the DNA molecule followed either by sliding [22–25] or direct intersegment transfer of the protein on DNA [22]. The values of bimolecular rate constants  $a_i$  used by other authors [13] were bounded by the “classical” diffusion limit, which may explain

Table 2

Parameter values used for numerical simulations of the deterministic and stochastic models

Reaction number	Deterministic model	Developed version of the stochastic model (see Table 1)
1	$v_s = 0.5 \text{ nM h}^{-1}$ $K_I = 2 \text{ nM}$ $n = 4$	$v_s = (0.5 \times \Omega) \text{ mol h}^{-1}$ , $a_1 = \Omega \text{ mol}^{-1} \text{ h}^{-1}$ , $d_1 = (160 \times \Omega) \text{ h}^{-1}$ , $a_2 = 10 \times \Omega \text{ mol}^{-1} \text{ h}^{-1}$ , $d_2 = (100 \times \Omega) \text{ h}^{-1}$ , $a_3 = 100 \times \Omega \text{ mol}^{-1} \text{ h}^{-1}$ , $d_3 = (10 \times \Omega) \text{ h}^{-1}$ , $a_4 = 100 \times \Omega \text{ mol}^{-1} \text{ h}^{-1}$ , $d_4 = (10 \times \Omega) \text{ h}^{-1}$
2	$v_m = 0.3 \text{ nM h}^{-1}$ $K_m = 0.2 \text{ nM}$	$k_{m1} = 165 \text{ mol}^{-1} \text{ h}^{-1}$ , $k_{m2} = 30 \text{ h}^{-1}$ , $k_{m3} = 3 \text{ h}^{-1}$ , $E_{m \text{ tot}} = E_m + C_m = (0.1 \times \Omega) \text{ mol}$
3	$k_s = 2.0 \text{ h}^{-1}$	$k_s = 2.0 \text{ h}^{-1}$
4	$v_1 = 6.0 \text{ nM h}^{-1}$ $K_1 = 1.5 \text{ nM}$	$k_{11} = 146.6 \text{ mol}^{-1} \text{ h}^{-1}$ , $k_{12} = 200 \text{ h}^{-1}$ , $k_{13} = 20 \text{ h}^{-1}$ $E_{1 \text{ tot}} = E_1 + C_1 = (0.3 \times \Omega) \text{ mol}$
5	$v_2 = 3.0 \text{ nM h}^{-1}$ $K_2 = 2.0 \text{ nM}$	$k_{21} = 82.5 \text{ mol}^{-1} \text{ h}^{-1}$ , $k_{22} = 150 \text{ h}^{-1}$ , $k_{23} = 15 \text{ h}^{-1}$ , $E_{2 \text{ tot}} = E_2 + C_2 = (0.2 \times \Omega) \text{ mol}$
6	$v_3 = 6.0 \text{ nM h}^{-1}$ $K_3 = 1.5 \text{ nM}$	$k_{31} = 146.6 \text{ mol}^{-1} \text{ h}^{-1}$ , $k_{32} = 200 \text{ h}^{-1}$ , $k_{33} = 20 \text{ h}^{-1}$ , $E_{3 \text{ tot}} = E_3 + C_3 = (0.3 \times \Omega) \text{ mol}$
7	$v_4 = 3.0 \text{ nM h}^{-1}$ $K_4 = 2.0 \text{ nM}$	$k_{41} = 82.5 \text{ mol}^{-1} \text{ h}^{-1}$ , $k_{42} = 150 \text{ h}^{-1}$ , $k_{43} = 15 \text{ h}^{-1}$ , $E_{4 \text{ tot}} = E_4 + C_4 = (0.2 \times \Omega) \text{ mol}$
8	$v_d = 1.5 \text{ nM h}^{-1}$ $K_d = 0.1 \text{ nM}$	$k_{d1} = 1650 \text{ mol}^{-1} \text{ h}^{-1}$ , $k_{d2} = 150 \text{ h}^{-1}$ , $k_{d3} = 15 \text{ h}^{-1}$ , $E_{d \text{ tot}} = E_d + C_d = (0.1 \times \Omega) \text{ mol}$
9	$k_1 = 2.0 \text{ h}^{-1}$	$k_1 = 2.0 \text{ h}^{-1}$
10	$k_2 = 1.0 \text{ h}^{-1}$	$k_2 = 1.0 \text{ h}^{-1}$

The reaction number refers to the corresponding lines in Table 1. In the last column, “mol” means molecule. In the developed stochastic model, when varying  $\Omega$  to modify the numbers of molecules involved in the circadian oscillatory mechanism, we wish to keep the number of gene promoter ( $G$ ) equal to unity without altering the relative weights of the different probabilities  $w_i$ , so as to keep dynamic behavior consistent with that predicted by the corresponding deterministic model governed by Eqs. (1)–(5). The numbers of enzyme molecules and the kinetic constants related to the steps involving  $G$  are therefore multiplied by  $\Omega$  in the last column that lists the parameter values for the detailed model. In the same column, to allow for cooperativity of the repression process, the parameters  $a_j$  and  $d_j$  ( $j = 1, \dots, 4$ ) which appear in steps 1a–h in Table 1, are chosen so that the dissociation constant  $K_j = d_j/a_j$  (with  $K_j^4 = \prod_{j=1}^4 K_j$ ) decreases as the number of molecules of  $P_N$  bound to the promoter increases. For simulations of the fully developed deterministic model governed by Eqs. (A.1)–(A.22) listed in appendix, parameter values are those given in the third column, with  $\Omega = 1$  and “mol” replaced by nM.

the absence of robust circadian oscillations reported in that work. As shown in the present study, indeed, at such lower values of  $a_j$  the oscillations are markedly affected by molecular noise, while robust circadian oscillations can occur with physiologically realistic, higher values of these kinetic parameters.

## Acknowledgements

We thank Dr. N. Barkai for discussions. This work was supported by grant no 3.4607.99 from the *Fonds de la Recherche Scientifique Médicale* (F.R.S.M., Belgium). DG is *Chargé de Recherches du Fonds National Belge de la Recherche Scientifique*.

## Appendix

The fully developed deterministic model, corresponding to the stochastic fully developed version of the core model for circadian rhythms, is governed by the following 22 differential equations, where quantities in brackets refer to complexes between the gene  $G$  and one or several molecules of repressor  $P_N$  (for consistency with respect to rate constants, units of  $G$  and of its complexes are expressed in nM):

$$\frac{dG}{dt} = -a_1 GP_N + d_1[GP_N], \quad (\text{A.1})$$

$$\frac{d[GP_N]}{dt} = a_1 GP_N - d_1[GP_N] - a_2[GP_N]P_N + d_2[GP_{N2}], \quad (\text{A.2})$$

$$\frac{d[GP_{N2}]}{dt} = a_2[GP_{N1}]P_N - d_2[GP_{N2}] - a_3[GP_{N2}]P_N + d_3[GP_{N3}], \quad (\text{A.3})$$

$$\frac{d[GP_{N3}]}{dt} = a_3[GP_{N2}]P_N - d_3[GP_{N3}] - a_4[GP_{N3}]P_N + d_4[GP_{N4}], \quad (\text{A.4})$$

$$\frac{d[GP_{N4}]}{dt} = a_4[GP_{N3}]P_N - d_4[GP_{N4}], \quad (\text{A.5})$$

$$\frac{dM}{dt} = v_s(G + [GP_N] + [GP_{N2}] + [GP_{N3}]) - k_{m1}ME_m + k_{m2}C_m, \quad (\text{A.6})$$

$$\frac{dE_m}{dt} = -k_{m1}ME_m + k_{m2}C_m + k_{m3}C_m, \quad (\text{A.7})$$

$$\frac{dC_m}{dt} = k_{m1}ME_m - k_{m2}C_m - k_{m3}C_m, \quad (\text{A.8})$$

$$\frac{dP_0}{dt} = k_s M - k_{11}P_0E_1 + k_{12}C_1 + k_{23}C_2, \quad (\text{A.9})$$

$$\frac{dE_1}{dt} = -k_{11}P_0E_1 + k_{12}C_1 + k_{13}C_1, \quad (\text{A.10})$$

$$\frac{dC_1}{dt} = k_{11}P_0E_1 - k_{12}C_1 - k_{13}C_1, \quad (\text{A.11})$$

$$\frac{dP_1}{dt} = -k_{21}P_1E_2 + k_{22}C_2 + k_{13}C_1 - k_{31}P_1E_3 + k_{32}C_3 + k_{43}C_4, \quad (\text{A.12})$$

$$\frac{dE_2}{dt} = -k_{21}P_1E_2 + k_{22}C_2 + k_{23}C_2, \quad (\text{A.13})$$

$$\frac{dC_2}{dt} = k_{21}P_1E_2 - k_{22}C_2 - k_{23}C_2, \quad (\text{A.14})$$

$$\frac{dP_2}{dt} = k_{33}C_3 - k_{41}P_2E_4 + k_{42}C_4 - k_{d1}P_2E_d + k_{d2}C_d - k_1P_2 + k_2P_N, \quad (\text{A.15})$$

$$\frac{dE_3}{dt} = -k_{31}P_1E_3 + k_{32}C_3 + k_{33}C_3, \quad (\text{A.16})$$

$$\frac{dC_3}{dt} = k_{31}P_1E_3 - k_{32}C_3 - k_{33}C_3, \quad (\text{A.17})$$

$$\frac{dE_4}{dt} = -k_{41}P_2E_4 + k_{42}C_4 + k_{43}C_4, \quad (\text{A.18})$$

$$\frac{dC_4}{dt} = k_{41}P_2E_4 - k_{42}C_4 - k_{43}C_4, \quad (\text{A.19})$$

$$\frac{dE_d}{dt} = -k_{d1}P_2E_d + k_{d2}C_d + k_{d3}C_d, \quad (\text{A.20})$$

$$\frac{dC_d}{dt} = k_{d1}P_2E_d - k_{d2}C_d - k_{d3}C_d, \quad (\text{A.21})$$

$$\begin{aligned} \frac{dP_N}{dt} = & -a_1GP_N + d_1[GP_N] - a_2[GP_{N1}]P_N + d_2[GP_{N2}] - a_3[GP_{N2}]P_N \\ & + d_3[GP_{N3}] - a_4[GP_{N3}]P_N + d_4[GP_{N4}] + k_1P_2 - k_2P_N \end{aligned} \quad (\text{A.22})$$

with  $G_{tot} = G + GP_N + GP_{N2} + GP_{N3} + GP_{N4} = 1$ .

## References

- [1] J.C. Dunlap, Cell 96 (1999) 271–290.
- [2] M.W. Young, S.A. Kay, Nature Rev. Genet. 2 (2001) 702–715.
- [3] S.M. Reppert, D.R. Weaver, Annu. Rev. Physiol. 63 (2001) 647–676.
- [4] P.E. Hardin, J.C. Hall, M. Rosbash, Nature 343 (1990) 536–540.
- [5] A. Goldbeter, Proc. R. Soc. Lond. B 261 (1995) 319–324.
- [6] A. Goldbeter, Biochemical Oscillations and Cellular Rhythms. The Molecular Bases of Periodic and Chaotic Behaviour, Cambridge University Press, Cambridge, UK, 1996.
- [7] J.-C. Leloup, A. Goldbeter, J. Biol. Rhythms 13 (1998) 70–87.
- [8] J.-C. Leloup, D. Gonze, A. Goldbeter, J. Biol. Rhythms 14 (1999) 433–448.
- [9] J.-C. Leloup, A. Goldbeter, BioEssays 22 (2000) 84–93.
- [10] J.-C. Leloup, A. Goldbeter, Proc. Natl. Acad. Sci. USA 100 (2003) 7051–7056.
- [11] H.R. Ueda, M. Hagiwara, H. Kitano, J. Theor. Biol. 210 (2001) 401–406.
- [12] P. Smolen, D.A. Baxter, J.H. Byrne, J. Neurosci. 21 (2001) 6644–6656.
- [13] N. Barkai, S. Leibler, Nature 403 (2000) 267–268.
- [14] D. Gonze, J. Halloy, A. Goldbeter, Proc. Natl. Acad. Sci. USA 22 (2002) 673–678.
- [15] D. Gonze, J. Halloy, A. Goldbeter, J. Biol. Phys. 28 (2002) 637–653.
- [16] D. Gonze, J. Halloy, J.-C. Leloup, A. Goldbeter, C.R. Biologies 326 (2003) 189–203.
- [17] D.T. Gillespie, J. Comput. Phys. 22 (1976) 403–434.
- [18] D.T. Gillespie, J. Phys. Chem. 81 (1977) 2340–2361.
- [19] J.M. Vilar, H.Y. Kueh, N. Barkai, S. Leibler, Proc. Natl. Acad. Sci. USA 99 (2002) 5988–5992.
- [20] D. Gonze, J. Halloy, P. Gaspard, J. Chem. Phys. 116 (2002) 10997–11010.
- [21] A.D. Riggs, S. Bourgeois, M. Cohn, J. Mol. Biol. 53 (1970) 401–417.
- [22] P.H. von Hippel, O.G. Berg, J. Biol. Chem. 264 (1989) 675–678.
- [23] B. Lewin, Genes V, Oxford University Press, Oxford, 1994.
- [24] G. Adam, M. Delbrück, in: A. Rich, N. Davidson (Eds.), Structural Chemistry and Molecular Biology, Freeman, New York, 1968, pp. 198–215.
- [25] P.H. Richter, M. Eigen, Biophys. Chem. 2 (1974) 255–263.